# Supplemental Material for "Enhanced tripartite interactions in spin-magnon-mechanical hybrid systems"

Xin-Lei Hei,[1] Peng-Bo Li,[1,2,*] Xue-Feng Pan,[1] and Franco Nori[2,3,4]

[1] *Ministry of Education Key Laboratory for Nonequilibrium Synthesis and Modulation of Condensed Matter, Shaanxi Province Key Laboratory of Quantum Information and Quantum Optoelectronic Devices, School of Physics, Xi'an Jiaotong University, Xi'an 710049, China*

[2] *Theoretical Quantum Physics Laboratory, RIKEN Cluster for Pioneering Research, Wako-shi, Saitama 351-0198, Japan*

[3] *RIKEN Center for Quantum Computing (RQC), 2-1 Hirosawa, Wako-shi, Saitama 351-0198, Japan*

[4] *Physics Department, The University of Michigan, Ann Arbor, Michigan 48109-1040, USA*

In this Supplemental Material, we first present more details about the three different schemes to realize the mechanical mode with a two-phonon driving. Then, we show how to realize the spin wave quantization in a magnetic microsphere. Finally, we show that the NV center, phonons, and magnons have a tripartite coupling in this hybrid setup. Some unfavorable factors such as driving defects, spin-rotation mode couplings, magnon-phonon interactions, and gas damping are considered and analyzed.

## A. MECHANICAL CENTER-OF-MASS VIBRATION

This section demonstrates theoretically the implementation of the mechanical center-of-mass vibration. To this end, we introduce three different proposals, i.e., a trapped diamond nanoparticle, a diamond cantilever, and a levitated micromagnet. We show that for all the schemes, the two phonon drive is easy to realize.

### a. Trapped diamond particles

The ion trap is used in this approach to achieve the levitation of diamond particles with NV centers [Fig. S1(a)]. Here, we investigate an electrical potential with a roughly quadrupolar spatial form in the trapping zone [1]. The potential can be written as

$$\Phi(x,y,z,t)=\frac{U_1}{2}(ax^2+by^2+cz^2)+\frac{U_2}{2}\cos(\omega_{\rm rf}t)(a'x^2+b'y^2+c'z^2), \tag{S1}$$

with the rf drive frequency $\omega_{\rm rf}$. According to Maxwell equations, the potential must always satisfy the Laplace equation, which leads to the constraint of coefficients as $a+b+c=0$ and $a'+b'+c'=0$. Otherwise, we assume that these coefficients are selected as $-(a+b)=c>0$ and $a'=-b'$, which causes static potential confinement for positively charged particles in the $z$ direction as well as dynamical confinement in the $x-y$ plane. Namely, we can treat the trapped particle as a linear oscillator along the $z$ axis, i.e., the Paul trap [2].

For the quantum-mechanical treatment of the center of mass motion in the trap, the time-independent potential can be written as

$$\hat{V}=\frac{1}{2}M\omega_{\rm m}^2\hat{z}^2, \tag{S2}$$

with the frequency

$$\omega_{\rm m}=\sqrt{\frac{cqU_1}{M}}. \tag{S3}$$

Here, $q$ is the charge and $M$ is the mass of the diamond particle. For the linear trap, the time-dependent part along $z$ axis could be eliminated with $c'=0$ [1]. However, for a particle in the harmonic trap, it is possible to add an oscillating potential $U_{\rm T}\cos(2\omega_{\rm p}t)$ with a voltage amplitude $U_{\rm T}$, which results in an external tunable drive

$$\hat{V}_{\rm dr}=-2qU_{\rm T}(\hat{z}/d_{\rm T})^2\cos(2\omega_{\rm p}t)$$

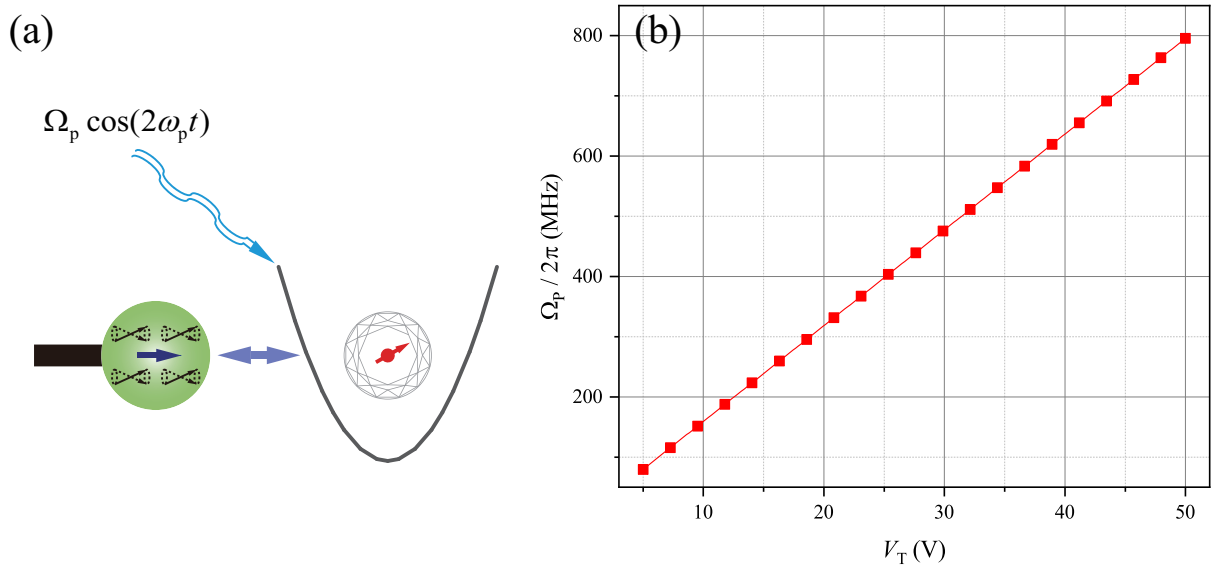


FIG. S1. (color online) (a) Schematic illustration of the proposal of the electrical trap for a diamond particle with single NV spins and a nearby YIG microsphere. (b) The driving frequency as a function of the voltage amplitude $U_T$ of the oscillating potential. Here, we assume the characteristic trap dimension $d_T = 100$ $\mu$m.

with a characteristic trap dimension $d_T$ [3, 4]. We then obtain a harmonic Hamiltonian with tunable stiffness as

$$\hat{H}_m = \frac{\hat{p}_z^2}{2M} + \frac{1}{2}M\omega_m^2\hat{z}^2 - \frac{1}{2}k_e(t)\hat{z}^2, \tag{S4}$$

with the time-dependent stiffness

$$k_e(t) = -\frac{4qU_T}{d_T^2}\cos(2\omega_p t). \tag{S5}$$

Employing the transformation $\hat{b} = \hat{z}/(2z_{zpf}) + iz_{zpf}\hat{p}_z/\hbar$ with $z_{zpf} = \sqrt{\hbar/(2M\omega_m)}$, the Hamiltonian of the mechanical mode can be written as (let $\hbar = 1$)

$$\hat{H}_m = \omega_m\hat{b}^\dagger\hat{b} - \Omega_p\cos(2\omega_p t)(\hat{b} + \hat{b}^\dagger)^2, \tag{S6}$$

with the parametric drive strength $\Omega_p = 2qU_T z_{zpf}^2/\hbar d_T^2$. In this scheme, the driving amplitude $\Omega_p/2\pi$ can reach the order of magnitudes $\sim 100$ MHz with the characteristic trap dimension $d_T = 100$ $\mu$m [see Fig. S1(b)], which is requisite for enhancing the tripartite interaction. For the levitation of diamond nanoparticles with NV centers, the rotation mode can be ignored, since the frequency of the rotation mode for spherical diamond is zero, which has been demonstrated in ref. [5].

### b. Diamond cantilevers

For this scheme, the NV center is embedded in a nano cantilever with the size $(l, w, t)$ as shown in Fig. S2. The vibration of the nano cantilever results in the relative motion between the NV center and the nearby micromagnet. In this case, the effective mass of the mechanical mode can be described as $M = \rho_c lwt/4$ with the mass density of cantilever $\rho_c$. The fundamental frequency can be estimated as

$$\omega_m = 3.516 \times (t/l^2)\sqrt{E/12\rho_c}$$

with Young's modulus $E$.

To modulate the motion of the cantilever, a pair of eletrodes are used [6]. One of them is coated on the lower surface of the cantilever. Another eletrode is placed just under the cantilever with a tunable time-varying voltage

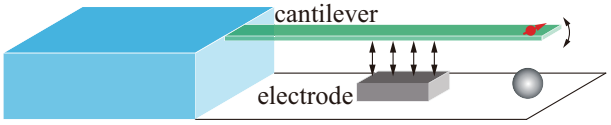


FIG. S2. (color online) Schematic of a mechanical cantilever with an NV center is coupled to a YIG sphere. The electrode (gray cube) provides the mechanical driving to enhance the tripartite interaction.

$V = V_0 + V_p \cos(2\omega_{\rm p} t)$. They can be regarded as a general parallel-plate capacitor with $C_r = \epsilon S/(d_0 + z)$. The spring constant of the cantilever can be modulated by the gradient of the electrostatic force $F = \partial(C_r V^2)/(2\partial z)$. Then, the mechanical mode with the electrical drive can be described as the Hamiltonian Eq. S6 as well, while the parametric-drive amplitude is

$$\Omega_{\rm p} = \frac{\epsilon S V_0 V_p z_{\rm zpf}^2}{\hbar d_0^2}. \tag{S7}$$

In this scheme, we consider a diamond cantilever with the dimensions $(l = 95, w = 0.02, t = 0.01)$ $\mu$m. Then the fundamental frequency can be estimated as $\omega_{\rm m} \sim 1$ kHz. The zero-point fluctuation is estimated as $z_{\rm zpf} \sim 5.6 \times 10^{-11}$ m. For the two-phonon drive, the aplitude $\Omega_{\rm p}/2\pi$ can reach the order of magnitudes $\sim 100$ MHz with the parameters: $V_0 = 10$ V,$V_p = 2$ V, $S = 5$ $\mu$m$\times 0.02$ $\mu$m, $d_0 \sim 300$ $\mu$m.

### c. Levitation of micromagnets

To levitate the magnets, one can place the YIG sphere above a type II superconductor [7]. The cooldown spanning the critical temperature $T_c$ generates a frozen dipole and an image dipole, which can supply a dynamic force to balance the gravity [Fig. S3(a)]. The potential function of the YIG sphere can be written as

$$U_{\rm m} = -\vec{\mu} \cdot \vec{B}_{\rm eff} + mgy, \tag{S8}$$

with the magnetic moment vector $\vec{\mu} = \mu_{\rm m} \vec{e}_z$, the effective field $\vec{B}_{\rm eff} = \vec{B}_{\rm frozen} + \vec{B}_{\rm image}/2$, and $g = 9.8$ m/s$^2$. Here, $\vec{B}_{\rm frozen}$ and $\vec{B}_{\rm image}$ denote the magnetic fields generated by the frozen dipole and the image dipole, respectively. Expanding the potential function at the equilibrium position, and removing the constant and high order components, the potential energy can approximate to a quadratic function of coordinates. Considering the vibration along the $z$ axis at the equilibrium height, the center-of-mass motion of the levitated micromagnet can be described by the Hamiltomian

$$\hat{H}_{\rm m}^{(0)} = \frac{\hat{p}_z^2}{2M} + \frac{1}{2} M \omega_{\rm m}^2 \hat{z}^2, \tag{S9}$$

with the momentum $\hat{p}_z$ and coordinate $\hat{z}$. These two terms are equivalent to a harmonic oscillator with the mass of micromagnet $M$ and the frequency $\omega_{\rm m}$. Here, the frequency can be expressed as

$$\omega_{\rm m} = \sqrt{\frac{3\mu_0}{4\pi M}} \frac{\mu_{\rm m}}{(h_{\rm eq} + h_{\rm cool})^{5/2}}. \tag{S10}$$

Here, the magnetic moment is defined as $\mu_{\rm m} = V M_{\rm s}$, with the volume $V$ and saturation magnetization $M$ of the YIG sphere. The distance from the superconductor to the YIG sphere during the cooldown process is denoted by $h_{\rm cool}$, while the equilibrium distance is denoted by $h_{\rm eq}$ in the above formula.

Then we introduce the electrical current next to the levitated YIG sphere as shown in Fig. S3(a). The magnetic field felt by the YIG sphere can be expressed as

$$\vec{B}_{\rm e} = \frac{\mu_0 I}{2\pi\sqrt{d_e^2 + z^2}} \vec{e}_z - \frac{\mu_0 I}{2\pi\sqrt{(d_e + 2h_{\rm eq})^2 + z^2}} \vec{e}_z, \tag{S11}$$

with the current $I = I_0 \cos(2\omega_{\rm p} t)$, the distance from the equilibrium of the YIG sphere to the electric wire $d_e$, the unit vector $\vec{e}_z$ parallel to the static external field, and the displacement of the micromagnet $z$. Note that the first term

in the above equation describes the field generated by the original electrical current, while the second term describes the field generated by the image current. Here, we assume the original current is much closer than the image current ($d_e \ll d_e + 2h_{\rm eq}$). The second term in Eq. S11, therefore, can be safely ignored, and the field can be simplified as

$$\vec{B}_{\rm e} \simeq \frac{\mu_0 I}{2\pi\sqrt{d_e^2+z^2}}\vec{e}_z. \tag{S12}$$

Then the magnetic interaction can be $U_{\rm drive} = -\vec{m}\cdot\vec{B}_{\rm e} = U_0 f(z)$ including the spatially invariant part $U_0 = -\mu_0 V M_{\rm s} I/(2\pi d_e)$ and the space-dependent function $f(z) = d_e/(d_e^2+z^2)^{1/2}$. Expanding this function at the equilibrium position ($z=0$) by Taylor series, we can rewrite the interaction potential as

$$U_{\rm drive} = U_0[f(0) + f'(0)z + \frac{1}{2}f''(0)z^2 + O(z)], \tag{S13}$$

where $O(z)$ denotes the sum of higher-order terms. Since the first term is constant, its effect on the dynamics of the system can be neglected. Note that the second term obviously vanishes for $f'(0)=0$. Consider the small vibration situation, we can safely ignore the higher-order terms $O(z)$. Then the magnetic interaction can be approximated as $U_{\rm drive} \simeq \frac{1}{2}U_0 f''(0)z^2$. Thus, we can obtain the driving Hamiltonian as $\hat{H}_{\rm m}^{(1)} = \frac{1}{2}k_{\rm e}(t)\hat{z}^2$. The effective time-dependent tunable stiffness coefficient is expressed as

$$k_{\rm e}(t) = -\frac{\mu_0 V M_{\rm s} I_0}{2\pi d_e^3}\cos(2\omega_{\rm p}t), \tag{S14}$$

with intensity $I_0$ and frequency $\omega_{\rm p}$. This term can supply the approach to modulate and drive the center-of-mass vibration via classical electrical current. Employing the destruction operator $\hat{b} = \hat{z}/(2z_{\rm zpf}) + iz_{\rm zpf}\hat{p}_z/\hbar$, the Hamiltonian of the mechanical mode can be written as

$$\hat{H}_{\rm m} = \hat{H}_{\rm m}^{(0)} + \hat{H}_{\rm m}^{(1)} = \omega_{\rm m}\hat{b}^\dagger\hat{b} - \Omega_{\rm p}\cos(2\omega_{\rm p}t)(\hat{b}+\hat{b}^\dagger)^2, \tag{S15}$$

with the driving amplitude $\Omega_p = \mu_0 V M_{\rm s} I_0 z_{\rm zpf}^2/(4\pi\hbar d_e^3)$. In this work, the driving amplitude $\Omega_{\rm p}/2\pi$ can reach $\sim 100$ MHz with proper parameters as shown in Fig. S3(a). Here, we can neglect the rotation mode of the levitated YIG sphere, when the large external magnetic field $B_{z,\rm K}$ is parallel to the initial magnetization direction of magnet. The conservation of total angular momentum restrains the mechanical rotation under the circumstances.

In practice, when the large external magnetic field $B_{z,\rm K}$ is not strictly parallel to the initial magnetization direction of the magnet, the rotation mode can appear with a frequency $\omega_r = \sqrt{\omega_{\rm K}\omega_{\rm I}}$. Here, $\omega_{\rm K} = |\gamma|B_{z,\rm K}$, being the magnon frequency on the order of magnitudes of 10 GHz. The Einsteinde Haas frequency is defined as $\omega_{\rm I} = \rho_{\rm spin}V_{\rm YIG}/(I_0\gamma)$, where $\rho_{\rm spin}$ is the spin density, $V_{\rm YIG}$ is volume of magnet, and $I_0 = 2\rho_{\rm YIG}V_{\rm YIG}R^2/5$ the moment of inertia with the mass density $\rho_{\rm YIG}$ and radius $R$ of the spherical magnet. In this work, the Einsteinde Haas frequency can be estimated as $\omega_{\rm I}/2\pi \sim 1.7$ kHz for the large spin density and the nanoscale of the YIG sphere. Then the frequency of rotation mode can be estimated as $\omega_r/2\pi \sim 4$ MHz, which results in a large detuning between the NV spin ($\omega_{\rm NV}/2\pi \sim 10$ GHz) and the rotation mode. Therefore, the coupling between the NV spin and the rotation mode can be safely neglected since they are far-off resonance in this scheme.

### d. The driving generated by imperfect current direction

For the levitation of magnets, we discuss the situation where the external current direction and the saturation magnetization are not strictly perpendicular in this section.

We assume that there is a small angle's deviation ($\theta$) between the external current direction and the saturation magnetization. Then the transverse component of magnetic field can be written as

$$\vec{B}_{\rm tr} = |\vec{B}_{\rm e}|\tan\theta(\cos\phi\vec{e}_x + \sin\phi\vec{e}_y), \tag{S16}$$

with an arbitrary angle $\phi$ in the plane $xOy$. For simplicity we let $\phi = 0$. Taking $U_{\rm tr} = -V\vec{\rm M}\cdot\vec{B}_{\rm tr}$ and $\hbar = 1$, this transverse field results in a driving of magnon as

$$\hat{H}_{\rm tr} = -\Omega_{\rm tr}\cos(2\omega_{\rm p}t)(\hat{a}+\hat{a}^\dagger), \tag{S17}$$

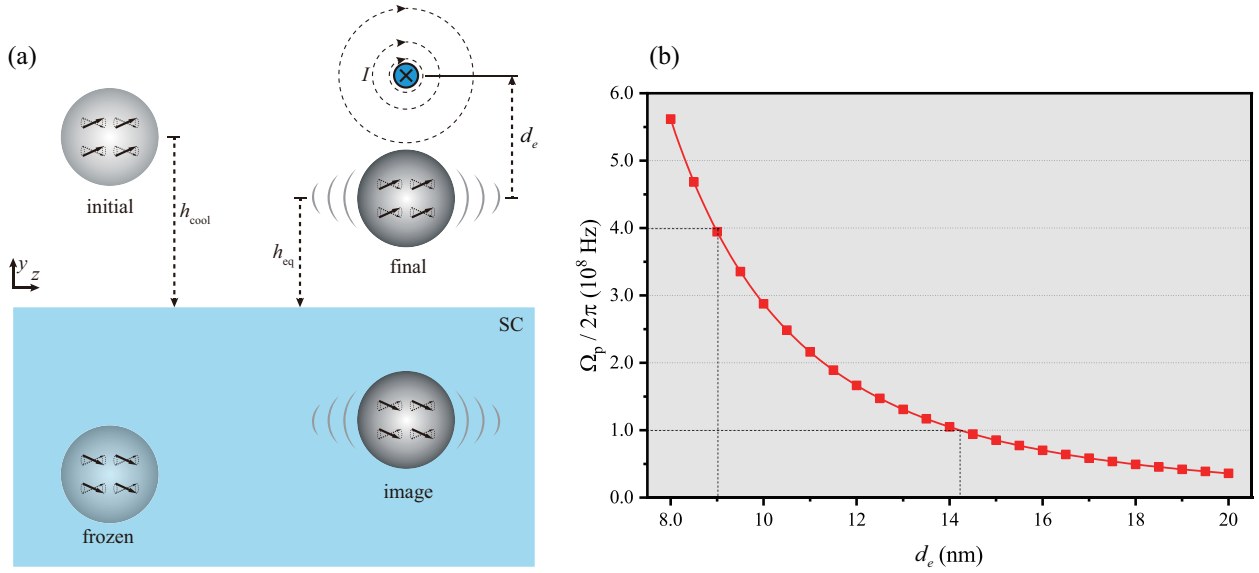


FIG. S3. (color online) (a) The driving frequency as a function of the distance from the equilibrium of the YIG sphere to the electric wire. Here, we assume the amplitude of the classical electricity $I_0 = 0.2$ mA. (b) Schematic of a YIG sphere attached to a mechanical cantilever is coupled to a NV center. The electrode (gray cube) provides the mechanical driving to enhance the tripartite interaction.

with the driving rate

$$\Omega_{\rm tr} = \frac{\mu_0 I_0 \tan\theta}{2\pi d}\sqrt{\frac{|\gamma| V M_s}{2\hbar}}. \tag{S18}$$

Besides, we consider the direct effect on Zeeman shift of the NV center caused by the current. Here, the current near the magnet generates the external magnetic induction, which results in the two-phonon drive of the mechanical mode. For the effect of NV spin, we assume that $r_{\rm NV}$ denotes the distance between the spin and the current. Applying $\hat{U}_{\rm Zeeman} = -g_e\mu_{\rm B}B_{e,z}\hat{\sigma}_z/2$ and $B_{e,z} = \mu_0 I_0 d/r_{\rm NV}^2$, the Zeeman shift of the NV center can be obtained as $\Delta\omega = g_e\mu_{\rm B}\mu_0 I_0 d/(2\hbar r_{\rm NV}^2)$. The shift then can be estimated as $\Delta\omega \sim 10$ MHz, which is far less than the frequency of the NV spin ($\sim 10$ GHz). Therefore, the direct effect on Zeeman shift of the NV center can be neglected in this scheme.

## B. QUANTIZATION OF THE SPIN WAVE

In this section, we demonstrate the quantization of the spin wave in a ferromagnetic microsphere. Then the magnon, the quanta of the SWs (spin waves), can be described with a theoretical model. First, we start from the general Landau-Lifshitz equation and simplify it under several physical approximations. Then, we show the Walker mode in a ferrite sphere in the second part. Finally, we obtain the bare Hamiltonian and quantization of the magnon modes, especially the Kittel mode.

### a. Spin wave equations in a magnetic sphere

Considering a continuous magnetization field $\vec{M}(\vec{r},t)$ with the corresponding eletromagnetic field intensity $\vec{E}(\vec{r},t)$ and $\vec{H}(\vec{r},t)$, the spin wave dynamics generally follows the Maxwell's equations with the relationship between the induced magnetization and the applied field. Then the dynamics of the magnetization satisfies the phenomenological Landau-Lifshitz equation as [8–10]

$$\frac{d}{dt}\vec{M}(\vec{r},t) = -|\gamma|\mu_0\vec{M}(\vec{r},t)\times\vec{H}_{\rm eff}(\vec{M},\vec{r},t). \tag{S19}$$

Here, the effective field $\vec{H}_{\rm eff}(\vec{M},\vec{r},t)$ includes the Maxwellian field $\vec{H}(\vec{r},t)$, the extra field $\vec{H}_{\rm ex}$, $\vec{H}_{\rm an}$, and $\vec{H}_{\rm dm}$ [8]. Here, the latter three parts depend on $\vec{M},\vec{r}$ and $t$. They are the effective fields on account of exchange, anisotropy, and dipole-dipole-interaction induced demagnetization, respectively. It indicates the inhomogeneity of this equation S19.

First, we suppose that the magnet is maximally magnetized along the $z$ axis ($\vec{e}_z$) by a collinear field. Compared with the saturated magnetization, the fluctuation deviating from the equilibrium is very small [11]. Thus, they can be defined as $\vec{M}(\vec{r},t)=M_S\vec{e}_z+\vec{m}(\vec{r},t)$ and $\vec{H}(\vec{r},t)=H_0\vec{e}_z+\vec{h}(\vec{r},t)$. Here, the dynamical variables satisfying $\vec{m}\ll M_S$ and $\vec{h}\ll H_0$ are to be solved. Associated with the domain wall interaction, the exchange field is less than the dipole-dipole interaction when the micromagnet size is much larger than the domain wall length. For a cubic material, the magnetocrystalline anisotropy can also be ignored [8, 9, 12]. As for the demagnetizing field in a spherical magnet, we reasonably suppose the expression $\vec{H}_{\rm dm}=-(M_S/3)\vec{e}_z$ [9, 13]. Combining the above settings with Eq. (S19) and neglecting the high order terms of variables $\vec{m}/M_S$ and $\vec{h}/H_0$, we can obtain the linearized Landau-Lifshitz equations as [8]

$$\begin{bmatrix} \dot{m}_x(\vec{r},t) \\ \dot{m}_y(\vec{r},t) \end{bmatrix} = \begin{bmatrix} -\omega_0 m_y(\vec{r},t)+\omega_M h_y(\vec{r},t) \\ \omega_0 m_x(\vec{r},t)-\omega_M h_x(\vec{r},t) \end{bmatrix}, \tag{S20}$$

where $m_x$ and $m_y$ denote the space components of $\vec{m}$, and the two relevant system frequencies are $\omega_{\rm M}=|\gamma|\mu_0 M_{\rm S}$ and $\omega_0=|\gamma|\mu_0(H_0-M_S/3)$.

In the end, we consider the magnetostatic approximation $\nabla\times\vec{h}(\vec{r},t)\simeq 0$. Under this circumstance, the electric field of the spin wave is decoupled to $\vec{h}$ according to the Maxwell equations. Then we can safely introduce the magnetostatic potential through $\vec{h}(\vec{r},t)=-\nabla\psi(\vec{r},t)$ due to the approximation. The zero-divergence condition $\nabla\cdot\vec{b}=0$ in Maxwell equations and the relation $\vec{b}=\mu_0(\vec{h}+\vec{m})$ make one to obtain the following equation [8]

$$\nabla^2\psi(\vec{r},t)=\partial_x m_x(\vec{r},t)+\partial_y m_y(\vec{r},t), \tag{S21}$$

which describes the situation inside the micromagnet with three acalar fileds $(\psi,m_x,m_y)$. For the case outside the micromagnet, the potential is limited $\nabla^2\psi=0$. Therefore, the spin wave can be completely described by the linear scalar equations Eq. (S20) and Eq. (S21) with the continuity of the normal direction components of $\vec{h}$ and $\vec{b}$. The spin-wave eigenmodes, solutions of the above scalar equations, are the magnetostatic dipolar spin waves which are called Walker modes as well [8, 9].

### b. Walker modes and Kittel modes

This section reveals the process of calculating the Walker modes. Introducing the eigenmodes, we can express the magnetization and magnetic fields as

$$\vec{m}(\vec{r},t)=\sum_\beta\left[s_\beta\vec{m}_\beta(\vec{r})e^{-i\omega_\beta t}+\text{c.c.}\right], \tag{S22a}$$

$$\vec{h}(\vec{r},t)=\sum_\beta\left[s_\beta\vec{h}_\beta(\vec{r})e^{-i\omega_\beta t}+\text{c.c.}\right]. \tag{S22b}$$

Here, the eigenmode fields $\vec{m}_\beta(\vec{r})$ and $\vec{h}_\beta(\vec{r})=-\nabla\psi_\beta(\vec{r})$ are characterized by a series of mode indices $\{\beta\}$, an eigenfrequency $\omega_\beta$ and a complex amplitude $s_\beta$ [14, 15]. Then the linearized Landau-Lifshitz equations turn to $i\omega m_x(\vec{r})=\omega_M\partial_y\psi(\vec{r})+\omega_0 m_y(\vec{r})$ and $i\omega m_y(\vec{r})=-\omega_M\partial_x\psi(\vec{r})-\omega_0 m_x(\vec{r})$, which are time-independent. We can eliminate the scalar field $m_x(\vec{r})$ and $m_y(\vec{r})$ through these equations and Eq. (S21). The formula merely contains the magnetostatic potential as

$$\nabla^2\psi_{\rm out}(\vec{r})=0, \tag{S23a}$$

$$(1+\chi_p)\left(\frac{\partial^2}{\partial x^2}+\frac{\partial^2}{\partial y^2}\right)\psi_{\rm in}(\vec{r})+\frac{\partial^2}{\partial z^2}\psi_{\rm in}(\vec{r})=0, \tag{S23b}$$

where $\psi_{\rm in}$ and $\psi_{\rm out}$ denote the magnetostatic potentials inside and outside the micromagnet, respectively. In this situation, we define the diagonal element of the Polder susceptibility tensor as $\chi_p(\omega)\equiv\omega_M\omega_0/(\omega_0^2-\omega^2)$ [8].

For the outside part, the general solution in the spherical coordinates can be written as

$$\psi_{\text{out}}(\vec{r}) = \sum_{lm}\left[\frac{A_{lm}}{r^{l+1}} + B_{lm}r^{l}\right]Y_l^m(\theta,\phi). \tag{S24}$$

Here, the boundary conditions determine the coefficients $A_{lm}$ and $B_{lm}$. Note that $Y_l^m(\theta,\phi)$ is the spherical harmonics. To solve the potential, a set of nonorthogonal coordinates $\{\xi,\eta,\phi\}$ is introduced. They fulfill $x = \sqrt{\chi_p}R\sqrt{\xi^2-1}\sin\eta\cos\phi$, $y = \sqrt{\chi_p}R\sqrt{\xi^2-1}\sin\eta\sin\phi$, and $z = \sqrt{\chi_p/(1+\chi_p)}R\xi\cos\eta$. Thus, the solution of Eq. (S23b) becomes available, which can be written as [14, 15]

$$\psi_{\text{in}}(\vec{r}) = \sum_{lm} C_{lm}P_l^m(\xi)Y_l^m(\eta,\phi), \tag{S25}$$

Each term of the above summation is a product of the boundary-conditions-dependent coefficient $C_{lm}$, Legendre polynomials, and spherical harmonics.

We then determine all the coefficients by the boundary conditions. First, to make the potential $\psi$ regular, the term corresponding to $B_{lm}$ should be removed since it is not convergent at infinity. That indicates the first condition, $B_{lm} = 0$. Considering the potential on the surface of the sphere, the coordinates are $\xi \to \xi_0 = \sqrt{(1+\chi_p)/\chi_p}$ and $\{\eta,\phi\} \to \{\theta,\phi\}$. Applying these coordinates to the two solution expressions Eq. (S24) and Eq. (S25), one can combine the normal-direction-component continuity of $\vec{h}$ ($\vec{b}$) and obtain the other two conditions

$$A_{lm} = C_{lm}P_l^m(\xi_0)R^{l+1}. \tag{S26}$$

$$\left.\frac{\partial\psi_{\text{out}}}{\partial r}\right|_{r=R} = \frac{\xi_0}{R}\left.\frac{\partial\psi_{\text{in}}}{\partial\xi}\right|_{r=R} - i\frac{\kappa_p}{R}\left.\frac{\partial\psi_{\text{in}}}{\partial\phi}\right|_{r=R}. \tag{S27}$$

Here, $\kappa_p(\omega) = \omega_M\omega/(\omega_0^2-\omega^2)$ is the off-diagonal element of the Polder susceptibility tensor [8]. Applying the above formulas, the Walker mode eigenfrequency fulfills the equation as [14, 15]

$$\xi_0(\omega)\frac{P_l'^m(\xi_0(\omega))}{P_l^m(\xi_0(\omega))} + m\kappa_p(\omega) + l + 1 = 0. \tag{S28}$$

There are two results we can obtain from this equation: (i) The frequency $\omega$ is independent $R$; (ii) Not all the solutions $\{l,m\}$ are positive and physical ($l = 0$, for example). One can use three indices $\{l,m,n\}$ to denote the $n$th eigenmodes of the spin waves. Several mode functions have been demonstrated in Fig. S4. In this work, the Kittel mode is the mode with the index (100). Note that some of the values of $l$ and $m$ are not included, since the solutions of corresponding equation are not positive and physical.

### c. The intrinsic Hamiltonian and quantization of the magnetostatic dipolar magnon modes

We now show the quantization of the Walker modes from a phenomenological micromagnetic energy functional [11]

$$E_m(\{\vec{m}\},\{\vec{h}\}) = \frac{\mu_0}{2}\int dV\vec{m}(\vec{r},t)\cdot\left[\frac{H_I}{M_S}\vec{m}(\vec{r},t) - \vec{h}(\vec{r},t)\right]. \tag{S29}$$

For convenience, we apply Eq. (S20) to the above expression. Then the energy becomes $E_m(\{\vec{m}\}) = 1/(2|\gamma|M_S)\times\int dV(m_x\partial_t m_y - m_y\partial_t m_x)$. Combining Eq. (S23a), one can transform the energy expression to $E_m = 1/(2\hbar|\gamma|M_S)\times\sum_\beta\hbar\omega_\beta\Lambda_\beta(s_\beta s_\beta^* + s_\beta^* s_\beta)$ with $\Lambda_\beta = 2\text{Im}\int dV m_{\beta y}m_{\beta x}^*$ [16, 17]. Compared with the Hamiltonian of the harmonic oscillator, we can choose adequate eigenmode normalization to fulfill $\Lambda_\beta = M_S|\gamma|\hbar$. Replacing the expansion coefficients with the bosonic magnon operators, i.e., $\{s_\beta, s_\beta^*\} \to \{\hat{s}_\beta, \hat{s}_\beta^\dagger\}$ with the commutation relation $[\hat{s}_\beta, \hat{s}_\beta^\dagger] = 1$, the quantized Hamiltonian can be written as $\hat{H}_m = \sum_\beta\hbar\omega_\beta[\hat{s}_\beta^\dagger\hat{s}_\beta + 1/2]$. Here, the constant term is the analogue of the zero-point energy. For simplicity, one can define a zero-point magnetization $M_{0\beta} = \sqrt{\hbar|\gamma|M_S/\tilde{\Lambda}_\beta}$ and the normalization constant $\tilde{\Lambda}_\beta = 2\text{Im}\int dV\tilde{m}_x^*\tilde{m}_y$. The mode functions, then, are replaced as $\{\vec{m}_\beta,\vec{h}_\beta\} \to M_{0\beta}\{\tilde{\vec{m}}_\beta,\tilde{\vec{h}}_\beta\}$. In the Schrdinger picture, the corresponding magnetization and magnetic field operators can be expressed as $\hat{\vec{m}} = \sum_\beta M_{0\beta}(\tilde{\vec{m}}_\beta\hat{s}_\beta + \text{H.c.})$ and $\hat{\vec{h}} = \sum_\beta M_{0\beta}(\tilde{\vec{h}}_\beta\hat{s}_\beta + \text{H.c.})$.

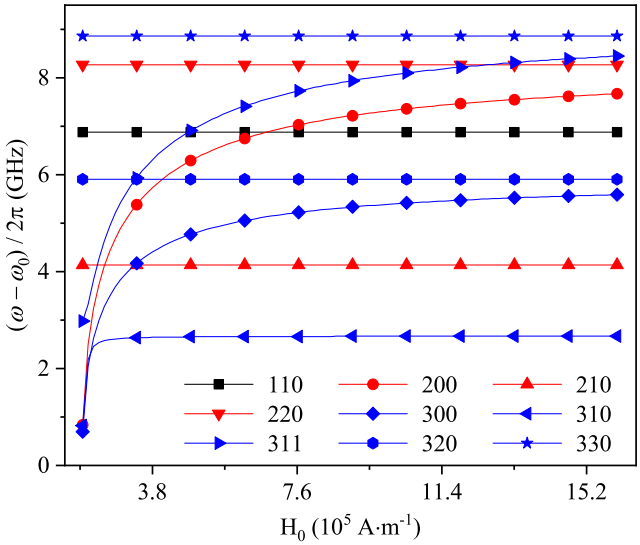


FIG. S4. (color online) The mode frequency as a function of the external magnetic field $H_0$. The number in legend indicate the indices $\{l, m, n\}$. The color of lines distinguishes the different index $l$.

As for the Kittel mode, the zero-point magnetization is $M_{\rm K} = \sqrt{\hbar|\gamma|M_{\rm S}/2V}$ with the saturation magnetization $M_{\rm S}$ and the volume $V$. The mode function, $\tilde{m}_K = \vec{e}_x + i\vec{e}_y$, depends on the coordinate vectors $\vec{e}_x$ and $\vec{e}_y$. The corresponding magnetization operator is

$$\hat{\vec{M}} = M_{\rm K}\left(\tilde{m}_{\rm K}\hat{a} + \tilde{m}^*_{\rm K}\hat{a}^\dagger\right). \tag{S30}$$

Here, we employ the annihilation (creation) operator of Kittel modes $\hat{a}$ ($\hat{a}^\dagger$). The Hamiltonian of Kittel modes can be written as

$$\hat{H}_{\rm K} = \omega_{\rm K}\hat{a}^\dagger\hat{a}, \tag{S31}$$

with the frequency $\omega_{\rm K} = |\gamma|B_z$ depending on the external static field.

### C. INTERACTION BETWEEN THE MAGNON AND THE CENTER OF MASS MOTION

In this section, we show the coupling between the magnon and the center of mass motion due to the magnetic field levitating the YIG magnet. The specific expression of the coupling rate are obtained with relevant theoretical derivation.

We start from the effective field levitating the YIG sphere in Eq. (S8). The field's component parallel to the $z$ axis cannot interact with Kittel mode, since its mode function in Eq. (S30) is transverse. We extract the left components of the effective field and obtain the effective magnetic field as

$$\vec{B}_{\rm tr} = -\frac{3\mu_0\mu_m}{4\pi r_{\rm f}^5}(h_{\rm eq} + h_{\rm cool})z\vec{e}_x, \tag{S32}$$

where we define that $r_{\rm f} = ((h_{\rm eq} + h_{\rm cool})^2 + z^2)^{1/2}$. Up to first order on the quantized coordinate $\hat{z} = z_{\rm zpf}(\hat{b} + \hat{b}^\dagger)$, we apply $\hat{H}_{\text{m-p}} = -\hat{\vec{\mu}}_M \cdot \hat{\vec{B}}_{\rm tr}$ with $\hat{\vec{\mu}}_M = V\hat{\vec{M}}$ to obtain the interaction Hamiltonian as

$$\hat{H}_{\text{m-p}} = g_{\text{m-p}}(\hat{b} + \hat{b}^\dagger)(\hat{a}^\dagger + \hat{a}), \tag{S33}$$

where the coupling rate is

$$g_{\text{m-p}} = \frac{\mu_0\mu_m V M_K z_{\rm zpf}}{4\pi\hbar(h_{\rm eq} + h_{\rm cool})^4}. \tag{S34}$$

### D. TRIPARTITE INTERACTION

In this section, we show the tripartite interaction in this hybrid quantum system. We start from the classical electromagnetism result that the field of a magnetic sphere with magnetization $\vec{M}$ can be described by

$$\vec{B}(\vec{r}) = \frac{\mu_0}{3}\frac{R^3}{r^3}\left[\frac{3(\vec{M}\cdot\vec{r})\vec{r}}{r^2} - \vec{M}\right]. \tag{S35}$$

Here, $\vec{B}(\vec{r})$ is the magnetic field at $\vec{r} = r_x\vec{e}_x + r_y\vec{e}_y + r_z\vec{e}_z$. In this work, we locate the NV center along the $z$ axis, which leads to $\vec{r} = r\vec{e}_z$. After introducing the quantized magnetization operator from Eq. (S30), we can obtain

$$\hat{\vec{M}} = M_{\mathrm{K}}\left[\left(\hat{a}+\hat{a}^\dagger\right)\vec{e}_x + i\left(\hat{a}-\hat{a}^\dagger\right)\vec{e}_y\right]. \tag{S36}$$

Applying the above expression to Eq. (S35), the magnetic field can be described by the operator expression

$$\hat{\vec{B}}(\vec{r}) = -\frac{\mu_0}{3}\frac{M_{\mathrm{K}}R^3}{r^3}\left[\left(\hat{a}+\hat{a}^\dagger\right)\vec{e}_x + i\left(\hat{a}-\hat{a}^\dagger\right)\vec{e}_y\right]. \tag{S37}$$

The interaction between the single NV center as a magnetic dipole and the magnetic field of the YIG sphere can naturally be described as $\hat{H}_{int} = -(g_e\mu_B/\hbar)\hat{\vec{B}}\cdot\hat{\vec{S}}$, with the Landé factor $g_e$, the Bohr magneton $\mu_B$ and the spin operator $\hat{\vec{S}} = (\hat{S}_x, \hat{S}_y, \hat{S}_z)$. In this work, the spin-operator components are defined as $\hat{S}_i = \hbar\hat{\sigma}_i/2$ with $i = x, y, z$, and the Pauli operators $\hat{\sigma}_i$ are defined in the basis $\{|g\rangle, |e\rangle\}$. Then, considering the center-of-mass relative motion between the NV center and the YIG sphere, the distance between them can be expressed as $r = r_0 + z$ with $r_0$ denoting the equilibrium part of the distance. Up to the first order of the coordinate $z$, we can quantize the center-of-mass vibration to obtain the interaction Hamiltonian as

$$\hat{H}_{\mathrm{int}} = \lambda(\hat{b}+\hat{b}^\dagger)(\hat{a}^\dagger\hat{\sigma}^- + \hat{a}\hat{\sigma}^+) + g_0(\hat{a}^\dagger\hat{\sigma}^- + \hat{a}\hat{\sigma}^+), \tag{S38}$$

with the tripartite coupling strength

$$\lambda = \frac{3g_e\mu_0\mu_B}{8\pi r_0^4}\sqrt{\frac{|\gamma|M_sV}{M\omega_{\mathrm{m}}}}, \tag{S39}$$

Here, $\mu_0$ is the permeability of vacuum, $M_{\mathrm{s}}$ is the saturation magnetization, and $V$ is the volume of YIG sphere. Otherwise, the pairwise coupling can be expressed as $g_0 = r_0\lambda/(3z_{\mathrm{zpf}})$. Then the total Hamiltonian can be written as

$$\begin{aligned}\hat{H} &= \hat{H}_{\mathrm{K}} + \hat{H}_{\mathrm{m}} + \hat{H}_{\mathrm{NV}} + \hat{H}_{\mathrm{int}} + \hat{H}_{\text{m-p}} \\ &= \omega_{\mathrm{K}}\hat{a}^\dagger\hat{a} + \omega_{\mathrm{m}}\hat{b}^\dagger\hat{b} + \frac{\omega_{\mathrm{NV}}}{2}\hat{\sigma}_z - \Omega_{\mathrm{p}}\cos(2\omega_{\mathrm{p}}t)(\hat{b}^{\dagger 2} + \hat{b}^2) + \lambda(\hat{b}+\hat{b}^\dagger)(\hat{a}^\dagger\hat{\sigma}^- + \hat{a}\hat{\sigma}^+) + \hat{H}_{\mathrm{JC}} + \hat{H}_{\text{m-p}},\end{aligned} \tag{S40}$$

Here, we denote the spin-magnon interaction with $\hat{H}_{\mathrm{JC}} = g_0(\hat{a}^\dagger\hat{\sigma}^- + \hat{a}\hat{\sigma}^+)$. For the driving due to the imperfect current direction in Eq. S17, the magnon frequency ($\sim 10$ GHz) is far from the frequency of it ($\sim 200$ MHz). Therefore, we can safely ignore it in the equation above. Using the rotating transformation $\hat{U}_0(t) = e^{-iH_0t}$ with $H_0 = \omega_{\mathrm{p}}(\hat{a}^\dagger\hat{a} + \hat{b}^\dagger\hat{b} + \hat{\sigma}_z/2)$ and dropping the the high frequency oscillation and the constant items, the above Hamiltonian can be simplified as

$$\hat{H}_{\mathrm{Total}} = \delta_{\mathrm{K}}\hat{a}^\dagger\hat{a} + \delta_{\mathrm{m}}\hat{b}^\dagger\hat{b} + \frac{\delta_{\mathrm{NV}}}{2}\hat{\sigma}_z - \frac{\Omega_{\mathrm{p}}}{2}(\hat{b}^{\dagger 2} + \hat{b}^2) + \lambda(\hat{b}+\hat{b}^\dagger)(\hat{a}^\dagger\hat{\sigma}^- + \hat{a}\hat{\sigma}^+) + \hat{H}_{\mathrm{JC}} + \hat{H}_{\text{m-p}}, \tag{S41}$$

The coefficients are defined as $\delta_{\mathrm{K}} = \omega_{\mathrm{K}} - \omega_{\mathrm{p}}$, $\delta_{\mathrm{m}} = \omega_{\mathrm{m}} - \omega_{\mathrm{p}}$, and $\delta_{\mathrm{NV}} = \omega_{\mathrm{NV}} - \omega_{\mathrm{p}}$. We then take the unitary transformation $\hat{U}_{\mathrm{S}}(r) = \exp[r(\hat{b}^2 - \hat{b}^{\dagger 2})/2]$ to diagonalize the center-of-mass mechanical mode. Here, the squeezing parameter $r$ is defined as $\tanh 2r = \Omega_{\mathrm{p}}/\delta_{\mathrm{m}}$. Therefore, we can obtain the total Hamiltonian as

$$\hat{H}^{\mathrm{S}}_{\mathrm{Total}} = \delta_{\mathrm{K}}\hat{a}^\dagger\hat{a} + \Delta_{\mathrm{m}}\hat{b}^\dagger\hat{b} + \frac{\delta_{\mathrm{NV}}}{2}\hat{\sigma}_z + \lambda_{\mathrm{eff}}(\hat{b}+\hat{b}^\dagger)(\hat{a}^\dagger\hat{\sigma}^- + \hat{a}\hat{\sigma}^+) + g_0(\hat{a}^\dagger\hat{\sigma}^- + \hat{a}\hat{\sigma}^+), \tag{S42}$$

where $\Delta_{\mathrm{m}} = \delta_{\mathrm{m}}/\cosh 2r$ and $\lambda_{\mathrm{eff}} = \lambda e^r$. Due to the amplification of the mechanical fluctuation caused by phonon squeezing, the tripartite coupling rate will be exponentially increased, while the bipartite coupling strength $g_0$ will remain unchanged. the tripartite interaction could be maintained at the same magnitude as the bipartite interaction. As shown in last section, the center of mass motion causes a change in the magnetic field, which causes the coupling

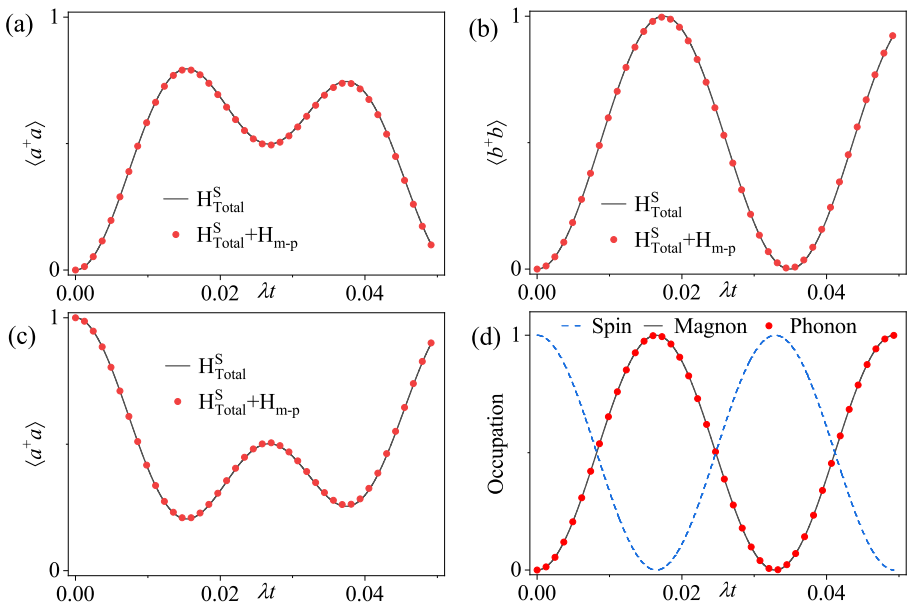


FIG. S5. (color online) The occupation of (a) magnon, (b) phonon, and (c) NV spin as function of time with Hamiltonian including the magnon-phonon parts $\hat{H}_{\text{m-p}}$ or not. (d) The time evolution of occupation of tripartite parts with initial state $|1,0,0\rangle$ under ideal conditions.

between the Kittel mode and mechanical mode. However, given the detuning between them ($\delta_{\text{K}} - \Delta_{\text{m}} \sim 10$ GHz) that is much larger than effective coupling rate ($e^r g_{\text{m-p}} \sim 10$ MHz), the interaction $\hat{H}_{\text{m-p}}$ can be disregarded. We show time evolution of occupations of the three subsystems in Fig. S5(a)-(c) to testify this approximation. For the tripartite interaction, there are two patterns of interaction depending on different resonance conditions. In this work, $g$ ($e$) denotes the $|0\rangle$ ($|+1\rangle$) state of the NV spin. The particle numbers of the phonons and magnons are denoted by $\{m, m\pm1\}$ and $\{k, k-1\}$. The condition with the red detuning, $\delta_{\text{K}} \simeq \delta_{\text{NV}} - \Delta_{\text{m}}$, allows for the interaction $\hat{a}\hat{b}\hat{\sigma}^+ + H.c.$ in the Hamiltonian (S42), which describes the spin and phonon annihilation upon magnon excitation and the inverse process. The other condition with the blue detuning, $\delta_{\text{K}} \simeq \delta_{\text{NV}} + \Delta_{\text{m}}$, allows for the interaction $\hat{a}^\dagger\hat{b}\hat{\sigma}^- + H.c.$, describing the spin annihilation with magnon and phonon excitation and the inverse process. We demonstrate the dynamical evolution of the spin, magnons, and phonons with the initial state $|1,0,0\rangle$ in Fig. S5(d).

We now consider the resonance condition with the blue detuned magnon in Hamiltonian (S42). Removing the off-resonance parts, the Hamiltonian is written as $\hat{H}_{\text{b}} = \delta_{\text{K}}\hat{a}^\dagger\hat{a} + \Delta_{\text{m}}\hat{b}^\dagger\hat{b} + (\delta_{\text{NV}}/2)\hat{\sigma}_z + \lambda_{\text{eff}}(\hat{a}^\dagger\hat{b}\hat{\sigma}^- + \hat{a}\hat{b}^\dagger\hat{\sigma}^+)$. Using the operator transformation $\hat{J}_- = \hat{a}\hat{b}^\dagger$, $\hat{J}_+ = \hat{a}^\dagger\hat{b}$ and $\hat{J}_z = (\hat{a}^\dagger\hat{a} - \hat{b}^\dagger\hat{b})/2$ [18], the above Hamiltonian can be rewritten as

$$\hat{H}_{\text{J-s}} \simeq \tilde{\omega}\hat{J}_z + \frac{\delta_{\text{NV}}}{2}\hat{\sigma}_z + \lambda_{\text{eff}}(\hat{J}_+\hat{\sigma}^- + \hat{J}_-\hat{\sigma}^+), \tag{S43}$$

where we define $\tilde{\omega} = \delta_{\text{K}} - \Delta_{\text{m}}$, and ignore the constant part $(\delta_{\text{K}} + \Delta_{\text{m}})\hat{N}/2$ with the magnon-phonon particle number operator $\hat{N} = \hat{a}^\dagger\hat{a} + \hat{b}^\dagger\hat{b}$. This Hamiltonian can be equivalent to the interaction between a 1/2 spin qubit and a N-spin ensemble with the total angular momentum $\hat{J}^2 = (\hat{N}/2)(\hat{N}/2+1)$. The eigenstates of $\{\hat{J}^2, \hat{J}_z\}$ can be described as $\{|N/2, j_s\rangle\}$ with the particle number operator eigenvalue $N$ and $j_s = -N/2, -N/2+1, ..., N/2$. Therefore, quantum applications based on the coupling between single spin and spin-ensemble can be realized with this tripartite system.

## E. GAS DAMPING

For the levitated nano particle, the gas damping should be considered as the main thermal decoherence of the mechanical mode. The collisions of gas molecules results in the effect, which can be described as [19]

$$\frac{\gamma_{\text{gas}}}{2\pi} = 3\eta\frac{a}{m}\frac{0.619}{0.619 + K_n}(1 + c_K), \tag{S44}$$

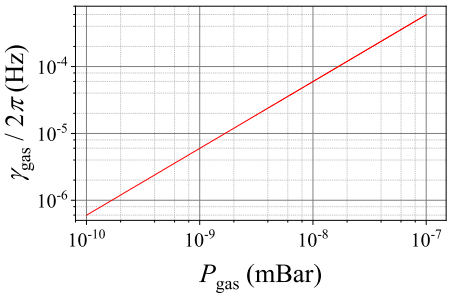


FIG. S6. (color online) The gas damping versus the pressure from $10^{-10}$ to $10^{-7}$ mBar. Here, the levitated diamond particle satisfies $R_s \sim 10$ nm.

with $c_K = 0.31K_n/(0.785 + 1.152K_n + K_n^2)$, the Knudsen number $K_n = \bar{l}/a$, the free mean path $\bar{l} \propto T_{\rm gas}/P_{\rm gas}$. Here, $T_{\rm gas}$ and $P_{\rm gas}$ are the temperature and the gas pressure. The gas damping is be proportional to the gas pressure in high vacuum as

$$\frac{\gamma_{\rm gas}}{2\pi} = 0.354\sqrt{\frac{m_{\rm gas}}{k_B T_{\rm gas}}}\frac{P_{\rm gas}}{a\rho}. \tag{S45}$$

Here, the characteristic size $a$ is the levitated particle's size, while $\rho$ is its mass density. Namely, $a = R_s$ for the scheme of levitated diamond particle. Taking levitated diamond scheme as an example, we show that the gas damping can reach the order of magnitudes $\sim 10^{-5}$ Hz to obtain a high Q-factor of $10^8$ with $\omega_{\rm m} \simeq 1$ kHz. The ultra-low pressure have been involved in ref. [20].

* lipengbo@mail.xjtu.edu.cn


[1] D. Leibfried, R. Blatt, C. Monroe, and D. Wineland, Quantum dynamics of single trapped ions, Rev. Mod. Phys. **75**, 281 (2003).

[2] W. Paul, Electromagnetic traps for charged and neutral particles, Rev. Mod. Phys. **62**, 531 (1990).

[3] D. J. Heinzen and D. J. Wineland, Quantum-limited cooling and detection of radio-frequency oscillations by laser-cooled ions, Phys. Rev. A **42**, 2977 (1990).

[4] W. Ge, B. C. Sawyer, J. W. Britton, K. Jacobs, J. J. Bollinger, and M. Foss-Feig, Trapped ion quantum information processing with squeezed phonons, Phys. Rev. Lett. **122**, 030501 (2019).

[5] T. Delord, L. Nicolas, Y. Chassagneux, and G. Hétet, Strong coupling between a single nitrogen-vacancy spin and the rotational mode of diamonds levitating in an ion trap, Phys. Rev. A **96**, 063810 (2017).

[6] P.-B. Li, Y. Zhou, W.-B. Gao, and F. Nori, Enhancing spin-phonon and spin-spin interactions using linear resources in a hybrid quantum system, Phys. Rev. Lett. **125**, 153602 (2020).

[7] J. Gieseler, A. Kabcenell, E. Rosenfeld, J. D. Schaefer, A. Safira, M. J. A. Schuetz, C. Gonzalez-Ballestero, C. C. Rusconi, O. Romero-Isart, and M. D. Lukin, Single-spin magnetomechanics with levitated micromagnets, Phys. Rev. Lett. **124**, 163604 (2020).

[8] D. D. Stancil and A. Prabhakar, *Spin Waves: Theory and Applications* (Springer, New York, 2009).

[9] A. Aharoni, *Introduction to the Theory of Ferromagnetism* (Clarendon Press, 2000).

[10] A. G. Gurevich and G. A. Melkov, *Magnetization oscillations and waves* (CRC press, 1996).

[11] N. Kostylev, M. Goryachev, and M. E. Tobar, Superstrong coupling of a microwave cavity to yttrium iron garnet magnons, Appl. Phys. Lett. **108**, 062402 (2016).

[12] H. Maier-Flaig, S. Klingler, C. Dubs, O. Surzhenko, R. Gross, M. Weiler, H. Huebl, and S. T. B. Goennenwein, Temperature-dependent magnetic damping of yttrium iron garnet spheres, Phys. Rev. B **95**, 214423 (2017).

[13] J. D. Jackson, *Classical electrodynamics* (John Wiley & Sons, 2007).

[14] P. C. Fletcher and R. O. Bell, Ferrimagnetic resonance modes in spheres, J. Appl. Phys. **30**, 687 (1959).

[15] P. Rschmann and H. Dtsch, Properties of magnetostatic modes in ferrimagnetic spheroids, Phys. Status Solidi B **82**, 11 (1977).

[16] D. Mills, Quantum theory of spin waves in finite samples, J. Magn. Magn. Mater. **306**, 16 (2006).

[17] L. R. Walker, Magnetostatic modes in ferromagnetic resonance, Phys. Rev. **105**, 390 (1957).

[18] S. Ding, G. Maslennikov, R. Hablützel, and D. Matsukevich, Quantum simulation with a trilinear Hamiltonian, Phys. Rev. Lett. **121**, 130502 (2018).

[19] S. A. Beresnev, V. G. Chernyak, and G. A. Fomyagin, Motion of a spherical particle in a rarefied gas. part 2. drag and thermal polarization, J. Fluid Mech. **219**, 10.1017/s0022112090003007 (2006).

[20] J. Gieseler, B. Deutsch, R. Quidant, and L. Novotny, Subkelvin parametric feedback cooling of a laser-trapped nanoparticle, Phys. Rev. Lett. **109**, 103603 (2012).